

INFLUENCE OF PARTICLE STRUCTURE CHANGES ON THE RATE OF COAL CHAR REACTION WITH CO_2

K. A. Debelak, M. A. Clark and J. T. Malito

Department of Chemical Engineering
Vanderbilt University
Nashville, TN 37235

Introduction

A common feature of gas-solid reactions is that the overall process involves several steps: (1) mass transfer of reactants and products from bulk gas phase to the internal surface of the reacting solid particle; (2) diffusion of gaseous reactants or products through the pores of a solid reactant; (3) adsorption of gaseous reactants on solid reactant sites and desorption of reaction products from solid surfaces; (4) the actual chemical reaction between the adsorbed gas and solid.

In studying gas-solid reactants, we are concerned with these four phenomena and other phenomena which affect the overall rate of reaction and performance of industrial equipment in which these gas-solid reactions are carried out. These other phenomena include: heat transfer, flow of gases and solids through reactors, and changes in the solid structure, all of which affect the rate of diffusion and surface area available for reaction. The reaction to be studied is the reaction between carbon and carbon dioxide to form carbon monoxide. This reaction is of importance for it is one of the prime reactions occurring in coal gasifiers, and also it is a reaction on which there is data from other investigations (1-17). Considerable discrepancy has been found for activation energies which ranges from 48-86 kcal/mol and for reaction rate constants. This can be explained by the somewhat oversimplified view of the mechanism which was thought to be rate-controlling, and the simplification made in the corresponding reaction rate models.

Gulbransen and Andrew (2) showed that the internal surface area of graphite increased during reaction with carbon dioxide and oxygen. Walker et al. (3) studied graphite rods for the possible correlations existing between reaction rates and changes in surface area during reaction. They concluded that the reaction develops new surface, to some extent, by enlarging the micropores of the solid but principally by opening up pore volume not previously available to reactant gas either because the capillaries were too small or because existing pores were unconnected. Surface area increased up to a point where rate of production of new surface equalled the destruction of old surface, after which surface area then continued to decrease. For the graphite-carbon dioxide reaction, Petersen (4) found that observed rates were not simple functions of the total available surface area as determined by low-temperature adsorptions prior to reaction, as might be expected if the reaction was chemical-reaction controlled.

Turkgodan et al. (18) studied the pore characteristics of several carbons, graphite, coke and charcoal. They concluded that about 1/2 of the volume is located in micropores and therefore not available for reaction. Most of the internal surface area was located in pores in the micropore range. The pore volume, pore surface area, and effective diffusivity increased with conversion during internal oxidation.

Dutta and Wen (16, 17) studied the reactivities of several raw coals and chars. They noted a change in the actual pore structures of a few samples at different conversions from scanning electron micrographs. A rate equation was proposed that incorporated the change of the relative available surface area during reaction. No measurements of this change were made. A rate expression, which includes the influence of a chemical and diffusion reaction controlling mechanisms, is expressed

$$\frac{dx_c}{dt} = \eta S k C_{CO_2} (1-x_c) \quad 1)$$

where:

- x_c is the conversion of the solid
- S is the surface area available for reaction
- k is the reaction rate constant
- η is the effectiveness factor
- C_{CO_2} is the concentration of CO_2 in gas phase
- t is time

The effectiveness factor η is equal to the ratio of the reaction rate under diffusion-controlled conditions to that which would occur if the concentration of reactants were equal to the surface concentration. For a first order diffusion-controlled reaction the influence of pore-diffusion is given by equation 2)

$$\eta = \frac{1}{\phi} \left[\frac{1}{\tanh 3\phi} - \frac{1}{3\phi} \right] \quad 2)$$

$$\phi = \frac{1}{3} r_c \left(S k / D_e \right)^{1/2} \quad 3)$$

where:

- S is the specific surface
- k is the reaction rate constant
- r_c is the radius of the particle
- D_e is the effective diffusivity

The effectiveness factor η is a function of the effective modulus, ϕ , which is dependent upon the effective diffusivity, D_e . The effective diffusivity and the surface area available for reaction change during the reaction.

This may be expressed as

$$S = S_0 f(X_c) \quad 4)$$

$$D_e = D_{e_0} h(X_c) \quad 5)$$

where S_0 and D_{e_0} are the available surface area and effective diffusivity at zero conversion, and $f(X_c)$ and $h(X_c)$ are functions of conversion, X_c . The determination of these changing parameters and their influence on the overall reaction rate is the objective of this research.

Effective Diffusivity

I. Theoretical Development of Model

Experimental determination of the effective diffusivity in coal is performed in a packed bed of coal particles with a carrier gas flowing through the bed. A pulse in the concentration of the adsorbate gas is introduced at the inlet of the packed bed. The mass transfer characteristics of the bed change the shape of the pulse as it passes through the bed. A theoretical model describing the mass transfer in the bed is used to relate the unsteady state concentration response in the bed effluent to the original pulse input. By applying the model to the experimental data, the parameters of the model are determined. The model describing the mass transfer in the packed bed consists of unsteady state material balances in the packed bed and the coal particles. Equations (6-14) describe the mass transfer in the packed bed of particles and the boundary conditions.

Material balance on coal particle

$$D_c \frac{\partial^2 q}{\partial r^2} + \frac{2}{r} \frac{\partial q}{\partial r} = \frac{\partial q}{\partial t} \quad 6)$$

Relation between adsorbed concentration and concentration of surface

$$q(r_c, t) = K_c C(r_c, t) \quad 7)$$

Boundary conditions

$$\frac{\partial q}{\partial r}(0, t) = 0 \quad 8)$$

$$\frac{3k}{r_c} \left[C(z, t) - C(r_c, t) \right] = \frac{\partial q}{\partial t} \quad 9)$$

$$\bar{q} = \frac{3}{r_c^3} \int_0^{r_c} r^2 q dr \quad 10)$$

Material balance on packed bed

$$D_L \frac{\partial^2 C}{\partial z^2} - v \frac{\partial C}{\partial z} - \frac{1 - \epsilon}{\epsilon} \frac{\partial \bar{q}}{\partial t} = \frac{\partial C}{\partial t} \quad 11)$$

Boundary conditions

$$C(z, 0) = C(r_c, 0) = q(r_c, 0) = 0 \quad 12)$$

$$C(0, t) = C_0 \delta(t) \quad 13)$$

$$C(\infty, t) = 0 \quad 14)$$

II. Solution of the Model

Three alternative techniques for solution and subsequent parameter estimation from the model are curve fitting in the time domain, curve fitting in the Laplace or Fourier domain, and the method of moments. Moments of the response curve resulting from a pulse input can be solved analytically for the solution to the model in the Laplace domain. Parameter estimation is achieved by matching the measured moments with the analytical expression for the moments. The method of moments was used in this work because it does not require a numerical solution to the model and because parameters estimation can be performed in the time domain. The Laplace transform is applied to the time variable in the equations and boundary conditions of the model. A system of coupled ordinary differential equations is obtained after applying this transform. A theorem relating the transformed solution to the absolute and central moments of time domain solution is

$$M_n = (-1)^n \lim_{s \rightarrow 0} \frac{d^n}{ds^n} \bar{C}(s, z) \quad 15)$$

The n^{th} absolute moment is defined as:

$$\mu_1' = \frac{M_1}{M_0} \quad 16)$$

$$M_n = \int_0^\infty t^n C(z, t) e^{-st} dt \quad 17)$$

The n^{th} central moment is defined by:

$$\mu_n = \frac{1}{M_0} \int_0^\infty (t - \mu_1')^n C(z, t) dt, \quad 18)$$

Applying equation 15) to the transformed solution of the model results in the following equations for the first absolute and second central moments:

$$\mu_1' = \frac{L}{v} \left[1 + \frac{(1 - \epsilon)}{\epsilon} K_p \right] \quad (19)$$

$$\mu_2 = \left[\frac{2D_c L}{v^3} + \frac{2L}{v} \frac{\epsilon}{(1 - \epsilon)} \left(\frac{r_c}{3k} - \frac{r_c^2}{15D_c K_p} \right) \right] \left[1 + K_p \frac{(1 - \epsilon)}{\epsilon} \right] \quad (20)$$

These two equations relate the model parameters to the moments which can be calculated from experimental data.

Experimental

WYODAK subbituminous coal, particle size 35 x 60, was used in the experimental study. The experimental system consisted of a pulse reactor, Figure 1, a flow type BET apparatus, Figure 2, and the chromatographic apparatus, Figure 3. This allowed determinations of surface area and effective diffusivity to be made in conjunction with reaction studies without removing the sample.

Measurements of surface area and effective diffusivity were made on raw coals. Surface area measurements were made by adsorbing carbon dioxide at 195 K for 30 minutes. The single point BET method was used for evaluation of the surface area. The raw coals were devolatilized by heating at 5°C/min to a temperature of 800°C to produce a coal char. Changes in surface area and effective diffusivity were again determined. The coal char was then partially reacted at a temperature of 800°C by injecting a known volume of carbon dioxide. Changes in surface area and effective diffusivity were again determined. This procedure was repeated until the conversion of the carbon in the coal approached 1.0.

Results and Discussion

The devolatilization caused structural changes which are reflected in an average weight loss of 41% of the initial weight, a decrease in the diffusion coefficient, and an increase in total surface area. Table 1 gives these changes for three WYODAK samples. The increase in surface area represents the opening of pores which were not accessible before devolatilization. Walls closing off pores are devolatilized and small pores inaccessible to the initial CO₂ adsorption are enlarged because of the evolution of volatile material during the heating. This new pore structure has a greater resistance to diffusion, seen as a decrease in the diffusion coefficient. The small pores and enlarged pore form a more complex network of voids within the particles. The production of char by devolatilization causes an increase in total available surface area and a decrease in the diffusion coefficient.

The heterogeneous chemical reaction causes continuous changes in the pore structure due to the consumption of carbon. Pore walls are being gasified slowly as the reaction continues toward completion. The continually changing internal structure affects the diffusion of gaseous reactants and products to and from the active carbon sites within the particle.

These phenomena may be described by examining Figure 4 which is a plot of the diffusion coefficient data for the three WYODAK samples measured at various carbon conversions. The diffusion coefficient increases slowly at low conversion and is somewhat stable during the mid-range of conversion, but increases very quickly as the reaction nears completion. Overall the diffusion coefficient increases as carbon conversion increases. These data can be correlated by

$$\frac{D_c}{r_c^2} = (0.06) \exp (1.7 \cdot X_c) \quad (21)$$

which gave an index of determination of 0.88. Physically, the pore structure after devolatilization consists of a small amount of void, characteristic of the low diffusion coefficient which means that the resistance to diffusion is substantial. During reaction these pores gradually enlarge due to gasification of the carbon. Therefore as conversion increases the pore volume or void increases resulting in less resistance to diffusion, which is reflected by the increase in the diffusion coefficient.

The CO₂-char reaction occurs at active carbon sites upon the coal char surface. Thus the consumption of the reactant carbon will affect the total surface area. The total surface area decreases for these WYODAK samples as the carbon conversion increases, Figure 5. As conversion goes toward completion, pore walls which are measured as surface area are gasified or consumed by the reaction causing a decrease in total surface area.

Figure 5 shows the specific surface area versus the carbon conversion. The specific surface area first goes through a minimum at low carbon conversions and then a maximum as carbon conversion goes toward completion. Mahajan and Walker (19) predicted the maximum in their qualitative description of the reaction process. Dutta and Wen (16) found that the reaction rate reaches a maximum at a carbon conversion of approximately 0.2 for reactions carried out at low temperatures. In an attempt to correlate this data they assumed a reaction rate model, Equation 1), for the chemical controlled regime. They incorporated into the model a proposed function of conversion which describes changes in surface area.

$$a = 1 + 100 X_c^{vB} \exp (-8X_c) \quad (22)$$

where a equals the specific surface area divided by the initial specific surface area. Fitting the model to the reaction rate versus conversion data the parameters of the proposed function were estimated by Dutta and Wen (16). This function describing changes in specific surface area exhibits a maximum at approximately the same conversion as our data. At low temperatures where reaction rate is predominantly chemically controlled, the maximum in the reaction rate vs. conversion data can be

explained by the fact that the specific surface for chemical reaction also goes through a maximum and this behavior of the specific area has been experimentally confirmed. The problem with equation 22) is that it predicts either a maximum or minimum for the value of a , but not both. In a recent paper Bhatia and Perlmutter (20), using a random pore model, have derived an expression for surface area as a function of conversion

$$a = \frac{1 - X}{\left(1 - \frac{r_c}{kCt}\right)^3} \sqrt{1 - \frac{4\pi L_0 (1 - \epsilon_0)}{s_0^2} \ln \left(\frac{1 - X}{\left(1 - \frac{r_c}{kCt}\right)^3}\right)} \quad (23)$$

where L_0 , S_0 and ϵ_0 are the initial total pore length, surface area to volume ratio, and porosity respectively. This equation correlates our data predicting both a minimum and maximum in values of specific surface area, Figure 6.

Acknowledgements

This work was supported by a National Science Foundation Research Institution Grant, Eng. 7907988.

References

- (1) Gadsby, J., Long, F. J., Sleighthorn, P., and Sykes, K. W., "The Mechanism of the Carbon Dioxide Reaction," Proc. Roy. Soc. London, Ser. A, 193, 377 (1948).
- (2) Gulbransen, E. A., and Andrew, K. F., "Reaction of Carbon Dioxide with Pure Artificial Graphite at Temperatures of 500°C," Ind. Eng. Chem., 44, 1039 (1952).
- (3) Walker, P. L., Foresti, R. J. and Wright, C. C., "Surface Area Studies of Carbon-Carbon Dioxide Reaction," Ind. Eng. Chem., 45, 8, 1703 (1953).
- (4) Petersen, E. E., Walker, P. L. and Wright, C. C., "Surface Area Development Within Artificial Graphite Rods Reacted with Carbon Dioxide from 900°C to 1300°C," Ind. Eng. Chem., 47, 1629 (1955).
- (5) Wicke, E., "Fifth Symposium on Combustion," p. 245, Reinhold, New York, New York (1955).
- (6) Rossberg, V. M., and Wicke, E., "Transportvorgänge und Oberflächenreaktionen bei der Verbrennung Graphitischen Kohlenstoff," Chem. Ing. Tech., 28, 191 (1956).
- (7) Ergun, S., "Kinetics of the Reaction of Carbon Dioxide with Carbon," J. Phys. Chem., 60, 480 (1956).

- (8) Walker, P. L., Rusinko, F., and Austin, L. G., "Gas Reactions Carbon," Advances in Catalysis, Vol. XI, 133-221 (1959).
- (9) Austin, L. G. and Walker, P. L., "Effect of Carbon Monoxide in Causing Nonuniform Gasification of Graphite by Carbon Dioxide," AIChE Journal, 9, 303 (1963).
- (10) Turkdogan, E. T., Kaoump, V., Vinters, J. V., "Rate of Oxidation of Graphite in Carbon Dioxide," Carbon, 6, 467 (1968).
- (11) Turkdogan, E. T., Vinters, J. V., "Kinetics of Oxidation of Graphite and Charcoal in CO₂," Carbon, 7, 101 (1969).
- (12) Yoshida, K., and Kinii, D., "Gasification of Porous Carbon by Carbon Dioxides," J. Chem. Engr., Japan, 2, 170 (1969).
- (13) Wen, C. Y., and Wy, N. T., "An Analysis of Slow Reactions in a Porous Particle," AIChE Journal, 20, 5, 833-840 (1974).
- (14) Walker, P. L., and Hippo, E., "Reactivity of Heat-Treated Coals in Carbon Dioxide at 900°C," Fuel, 54, 245 (1975).
- (15) Fuchs, W., Yavarsky, P. M., "Am. Chem. Soc., Div. Fuel Chem.," 20 (3), 115, (1975).
- (16) Dutta, S., Wen, C. Y., "Reactivity of Coal and Char. 2. In Oxygen-Nitrogen Atmosphere," Ind. Eng. Chem., Process Des. Dev., 16, No. 1, 20 (1977).
- (17) Dutta, S., Wen, C. Y., "Reactivity of Coal and Char. 2. In Oxygen-Nitrogen Atmosphere," Ind. Eng. Chem., Process Des. Dev., 16, No. 1, 31 (1977).
- (18) Turkdogan, E. T., Olsson, R. G., and Vinters, J. V., "Pore Characteristics of Carbon," Carbon, 8, 545-564 (1970).
- (19) Mahajan, A. P., Yarzab, R., and Walker, P. L., Jr., "Unification of Coal-Char Gasification Reaction Mechanisms," Fuel, Vol. 57, pp. 643-646, October 1978.
- (20) Bhatia, S. K. and Perlmutter, D. D., "A Random Pore Model for Fluid Solid Reactions: I. Isothermal, Kinetic Control", AIChE J., 26, No. 3, 379-385 (1980).

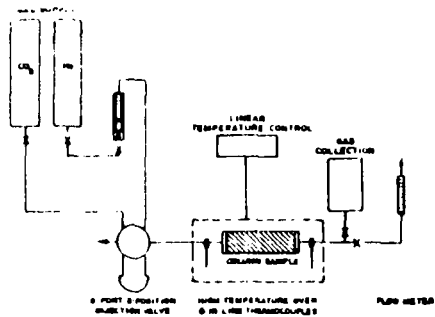


Figure 1 Schematic Diagram of the Apparatus for Reaction of Coal and CO_2 at high Temperatures

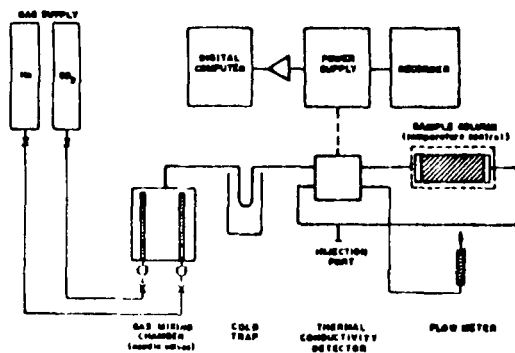


Figure 2 Schematic Diagram of the Experimental Apparatus for Determination of B.E.T. Surface Area

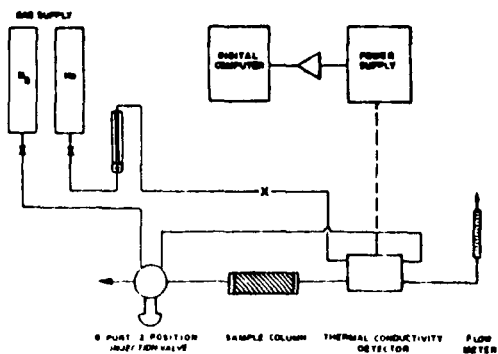


Figure 3 Schematic Diagram of Experimental Apparatus for Determination of Effective Diffusivity

TABLE 1

EFFECTS OF DEVOLATILIZATION

WTODAK	Weight (g) (coal)/(char)	Total Surface (m ²) (coal)/(char)	Specific Surface Area (m ² /g) (coal)/(char)	Diff. Co. (s ⁻¹) (coal)/(char)
Sample 1	1.0094/0.6172	80.9/128.0	80.15/207.4	8.214/8.8438
Sample 2	0.9719/0.5712	70.9/104.5	72.9/182.9	1.158/8.8664
Sample 3	1.0169/0.5910	74.7/102.6	71.9/171.6	1.476/8.8719

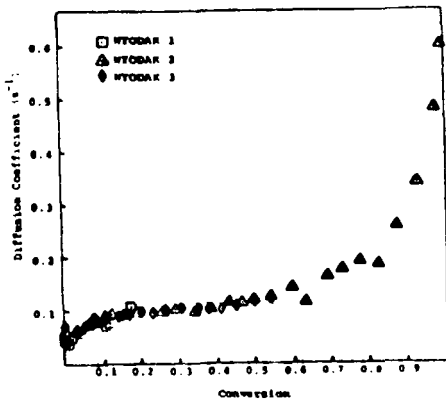


Figure 4 Diffusion Coefficient versus Conversion

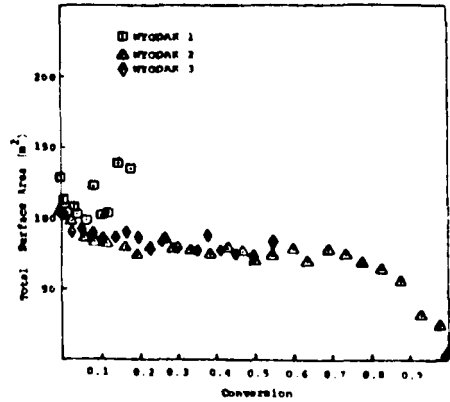


Figure 5 Total Surface Area Versus Conversion

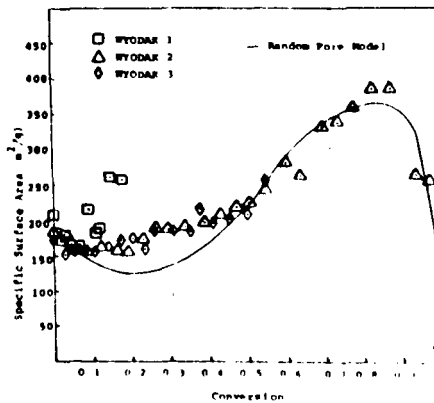


Figure 6 Comparison Between Experimental Specific Surface Area and Prediction of Random Pore Model